Experimental evidence for the formation of cationic intermediates during iodine(III)-mediated oxidative dearomatization of phenols

Journal:	*Organic & Biomolecular Chemistry*
Manuscript ID	OB-COM-07-2018-001652.R3
Article Type:	Communication
Date Submitted by the Author:	30-Aug-2018
Complete List of Authors:	Tang, Ting; Texas Tech University, Department of Chemistry & Biochemistry Harned, Andrew; Texas Tech University, Department of Chemistry & Biochemistry

Journal Name

COMMUNICATION

Experimental evidence for the formation of cationic intermediates during iodine(III)-mediated oxidative dearomatization of phenols

Received 00th January 20xx,
Accepted 00th January 20xx

DOI: 10.1039/x0xx00000x

www.rsc.org/

Ting Tang[a] and Andrew M. Harned *[a]

Iodine(III)-based oxidants are commonly used reagents for the oxidative dearomatization of phenols. Having a better understanding of the mechanism through which these reactions proceed is important for designing new iodine(III)-based reagents, catalysts, and reactions. We have performed a Hammett analysis of the oxidative dearomatization of substituted 4-phenylphenols. This study confirms that iodine(III)-mediated oxidative dearomatizations likely proceed through cationic phenoxenium ions and not the direct addition of a nucleophile to an iodine-bound phenol intermediate.

Phenyliodine(III) diacetate (PIDA) and its congeners are powerful organic oxidants that have been employed in a wide range of interesting transformations.[1] One of the more common applications of these reagents is in the oxidative dearomatization of phenols to give cyclohexadienones (e.g., **1**→**3**, Figure 1).[2] Curiously, despite the wide use of this transformation, its mechanistic details are shrouded in mystery. It is widely accepted that there is an initial ligand exchange between phenol **1** and PIDA to generate an intermediate aryl-λ^3-iodane (**2**). What happens next is subject to some debate, and two mechanistic proposals are usually encountered in the literature.[3] One involves a bimolecular redox decomposition pathway (Path A, **2**→**3**) in which a nucleophile (in this case R^2OH) attacks the aromatic ring of the "activated" phenol.[4] This S_N2'-like mechanism is proposed to directly form dienone **3** through a single transition state. Alternatively, aryl-λ^3-iodane **2** follows a unimolecular redox decomposition pathway (Path B, **2**→**4**→**3**). This S_N1-like mechanism involves forms phenoxenium ion **4**,[5] which is then rapidly trapped by the nucleophile to give dienone **3**.

Although pathways A and B both result in the same product, having a better understanding of how these reactions proceed is important for the development of new reactions. Answering this mechanistic question is also of critical importance for developing next generation chiral aryl iodide catalysts.[6,7,8] Trying to design a chiral environment around an intermediate that reacts through a unimolecular pathway is a very different challenge than one involving a bimolecular pathway.

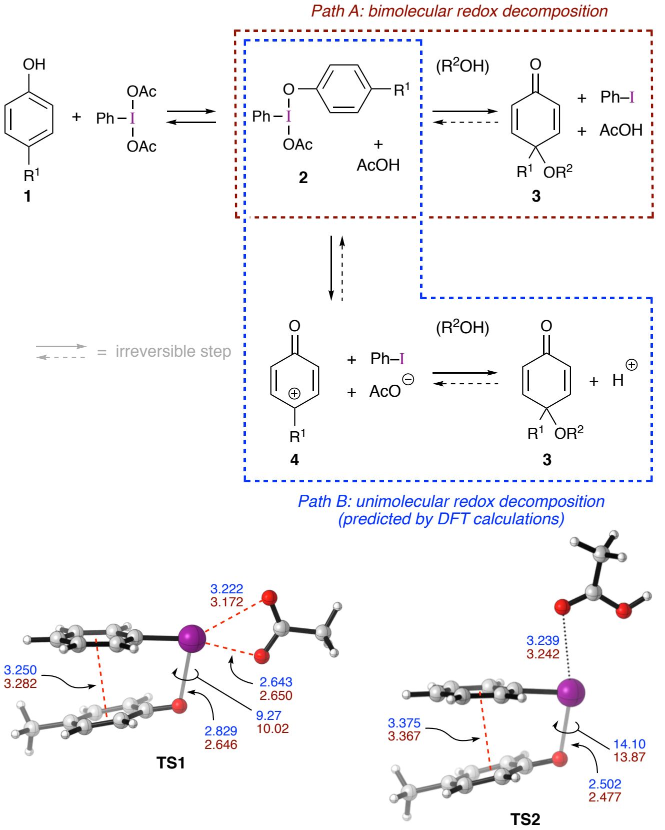

Figure 1. Mechanistic picture for iodine(III)-mediated oxidative dearomatizations.

Recently, we reported a series of DFT calculations, using water as a nucleophile, aimed at probing the likelihood of pathways A and B.[9] Briefly, we were able to locate transition states (**TS1** and **TS2**, Figure 1) corresponding to the unimolecular redox decomposition of iodane **2**. Transition state **TS2**, in which the acetate group of iodane **2** is protonated, represents an attempt account for potential hydrogen bonding effects[10] during the decomposition of the

---

[a] *Texas Tech University, Department of Chemistry & Biochemistry, 1204 Boston Ave., Lubbock, TX, 79409-1061, United States, Email: andrew.harned@ttu.edu*

Electronic Supplementary Information (ESI) available: Experimental procedures, characterization data, tabulated energies, coordinates, and graphical structures of all relevant structures. See DOI: 10.1039/x0xx00000x iodane and is lower in energy ($\Delta G^{\ddagger}_{TS1}$ ~29 kcal/mol; $\Delta G^{\ddagger}_{TS2}$ ~10 kcal/mol). In contrast, we were unable to locate a transition state representing the direct addition of a nucleophile (H_2O) to the phenolic ring of iodane **2**. The reason for this failure was attributed to the overall negative charge of the phenolic portion of iodane **2** and the ability of this partial negative charge to repel an incoming nucleophile. These results strongly suggested that path B was not only the favored pathway for the decomposition of iodane **2**, but was likely the *only* productive pathway available.[11] Although these results put a crack in the mechanistic black box, we recognized that a more substantial experimental result was needed in order to give weight to this prediction. Herein, we report such a result.

Based on the computational prediction that these reactions proceed through a phenoxenium ion, we reasoned that a Hammett study[12] of the oxidative dearomatization of substituted 4-phenylphenols (**5**→**6**)[13] would be an ideal solution (Figure 2A). However, the rapid reaction rates typically seen during iodine(III)-mediated oxidative dearomatization reactions preclude the measurement of individual rate constants by traditional means. Instead, we turned to the "one-pot" method reported by Harper,[14] in which the necessary relative rates (k_X/k_H) are obtained using a competition experiment[15] and are related, by equation 1, to the amount of each compound present at the beginning of the experiment and at the time of the analysis. Compared to traditional methods of obtaining rate data, this model has many practical benefits,[14] not least of which is that accurate measurements of substrate or product concentrations is not necessary. Only the ratio at the beginning and end of the reaction is needed.

$$\frac{k_X}{k_H} = \frac{\ln(\frac{s_X}{s_{X,t=0}})}{\ln(\frac{s_H}{s_{H,t=0}})} \qquad (1)$$

In our study,[16] naphthalene was used as an internal standard to measure the ratio (by HPLC) of phenols **5a** and **5b-g** at the beginning and end of the reaction. Each reaction was run to partial conversion, by using a limiting amount of PIDA, in order to ensure some of each starting material remained. The resulting Hammett plots, with respect to σ_p, σ^+, and σ^- values,[17] are shown in Figure 2B. As can be seen, plotting against σ^+ gave the best linear fit. The plots using σ_p and σ^- both displayed significant curvature. Importantly, the linear fit for all three of the plots returned negative ρ values, which is consistent with the development of positive charge in the phenolic ring of iodane **2** during the rate determining step.

In order to gauge whether resonance or inductive effects are more important, we plotted the relative rate data against σ_R and σ_I values[17] (Figure 2C). Neither gave a very good correlation (R^2 value), but visual inspection of the σ_I plot reveals it is very scattered, compared to the corresponding σ_R plot. Resonance effects are expected to be more important for stabilizing/destabilizing a developing charge, but will not be as important for nucleophilic attack on a "neutral" molecule. Our results also show that the methoxy substituent, a resonance donating group, facilitates the reaction. It is difficult to imagine how such a group would facilitate direct, nucleophilic attack onto iodane **2**. In contrast, strongly electron-withdrawing groups like CF_3 and CO_2Et slow the reaction rate. Again, it is difficult to imagine how an electron-withdrawing group would be detrimental to a reaction mechanism that involves direct addition of a nucleophile to iodane **2**.

Comparing our results to literature reports of relevant reactions was quite instructive. Hammett plots for the ionization of phenols (ρ = +1.819–3.197) and anilinium ions (ρ = +2.767–3.558)[18] have positive ρ values. This indicates that our results are not a direct measure of the stabilization/destabilization of the partial negative charge in iodane **2**. We are aware of only one other Hammett study involving an iodine(III)-mediated oxidation. This report used substituted phenyliodine(III) diacetates [$RC_6H_4I(OAc)_2$] for the oxidative cleavage of vicinal diols.[19] The resulting Hammett plot had a positive slope (ρ = +1.475 vs σ). This result is consistent with a reaction in which the iodine center is reduced (iodine become less positive). A ρ value of opposite sign should be expected when monitoring the oxidation of a substrate.

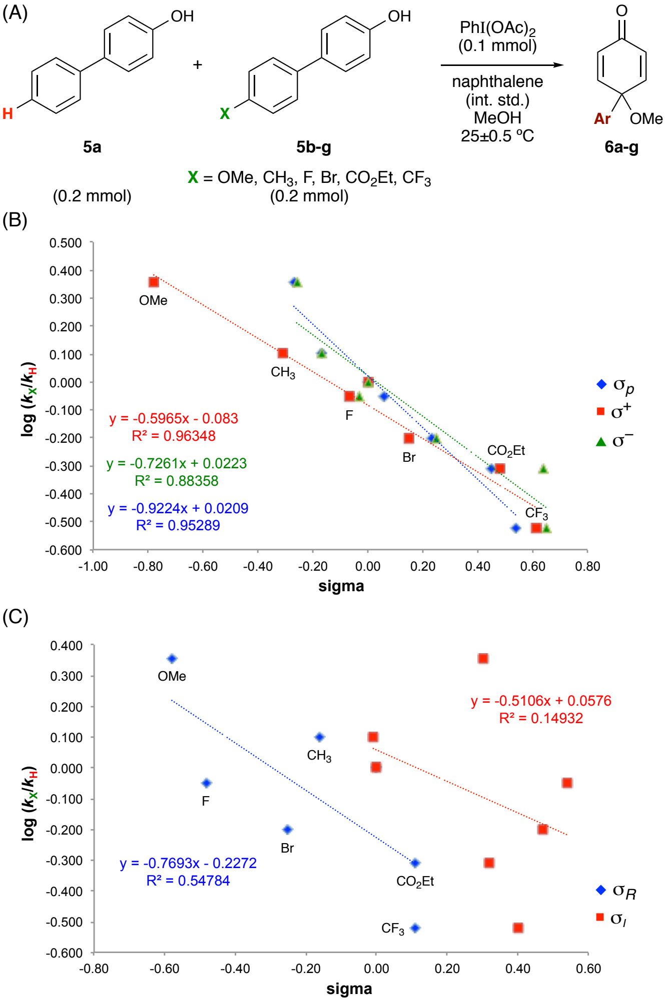

Figure 2. (A) Competition experiment used to measure relative rate data. (B) Hammett plots of relative rate data. (C) Evaluation of resonance and inductive effects on relative rates.

We also performed a series of DFT calculations in order to further corroborate our experimental results.[16] For this work we made use of the relationship between the Hammett equation and free energy (e.g., equation 2).[20] First, we determined the overall free energy change for the conversion of phenols **5a-g** to the phenoxenium ions **7a-g** (Figure 3A). Plotting the free energy changes against σ_p, σ^+, and σ^-

returned negative ρ values in all cases. As should be expected, the best correlation was seen when σ^+ was used.[16]

$$\log\frac{k_X}{k_H} = \frac{-\Delta G_X^\ddagger}{2.3RT} + \frac{\Delta G_H^\ddagger}{2.3RT} = \sigma\rho \quad (2)$$

Next we plotted the calculated $\Delta G^\ddagger$ values for the protonated unimolecular transition states (e.g., **TS2**). Once again (Figure 3B), negative ρ values were returned in all cases. Although the correlation with σ^+ was not as good in this case, visual inspection reveals the plot is more linear than those for σ_p and σ^-. Importantly, the plots for σ_p and σ^- have a curvature that is very similar to that seen when plotting our experimental results.[21] This suggests that while our transition state model may not be completely accurate, it is a good approximation of what occurs in the flask. Any discrepancies are likely due to our handling of the protonation state of the intermediate aryl-λ^3-iodanes (**2**) and the unimolecular redox decomposition transition state (**TS1** vs. **TS2**).

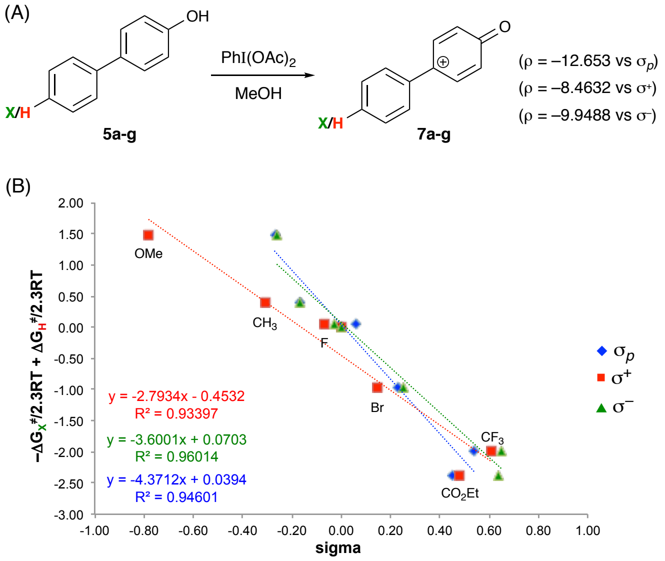

Figure 3. (A) ρ values of the Hammett plots (see ESI) for the conversion of phenols into phenoxenium ions using calculated free energy changes. (B) Hammett plots using calculated transition state energies (ΔG‡).

In conclusion, we have performed a detailed Hammett analysis of iodine(III)-mediated oxidative dearomatizations of phenols. Our analysis indicates the reaction likely proceeds through a mechanism in which a positive charge develops on the phenol during the rate determining step. This is consistent with a unimolecular redox decomposition pathway (Figure 1, path B) and is not consistent a bimolecular redox decomposition pathway (Figure 1, path A). These findings have significant implications with regard to the design of future aryl iodide catalysts and reagents, as well as new iodine(III)-mediated reactions involving phenols.

Acknowledgements

Financial support for this work provided by Texas Tech University and the National Science Foundation (CHE-1541685). We are grateful to Prof. David Birney (Texas Tech) for helpful discussions and suggestions.

Conflicts of interest

There are no conflicts to declare.

Notes and references

1 (a) *Hypervalent Iodine Chemistry: Modern Developments in Organic Synthesis*, ed.: T. Wirth, Springer, Berlin, 2003. (b) V. V. Zhdankin, *Hypervalent Iodine Chemistry*, Wiley, West Sussex, 2014.
2 Reviews: (a) A. Pelter and R. S. Ward, *Tetrahedron*, 2001, **57**, 273; (b) R. M. Moriarty and O. Prakash, *Org. React.*, 2001, **57**, 327; (c) S. Quideau, L. Pouysegu, and D. Deffieux, *Synlett*, 2008, 467; (d) L. Pouysegu, D. Deffieux, and S. Quideau, *Tetrahedron*, 2010, **66**, 2235; (e) S. Quideau, L. Pouysegu, P. A. Peixoto, and D. Deffieux in *Hypervalent Iodine Chemistry*, ed: T. Wirth, Springer, Berlin, 2016, pp. 25–74.
3 Sometimes a radical pathway is invoked. However, Kita has shown that such a mechanism only applies to oxidations of aryl *ethers* and requires very specific conditions. See: (a) Y. Kita, H. Tohma, K. Hatanaka, T. Takada, S. Fujita, S. Mitoh, H. Sakurai, and S. Oka, *J. Am. Chem. Soc.*, 1994, **116**, 3684; (b) H. Tohma, H. Morioka, S. Takizawa, M. Arisawa, and Y. Kita, *Tetrahedron*, 2001, **57**, 345; (c) T. Dohi, M. Ito, N. Yamaoka, K. Morimoto, H. Fujioka, and Y. Kita, *Tetrahedron*, 2009, **65**, 10797; (d) reference 1a, pp 44 and 1b, pp 15.
4 Reference 1b, pp 184.
5 Phenoxenium ions have also been implicated in anodic oxidations of phenols. See: J. S. Swenton, K. Carpenter, Y. Chen., M. L. Kerns, and G. W. Morrow, *J. Org. Chem.*, 1993, **58**, 3308.
6 A. M. Harned, *Tetrahedron Lett.* 2014, **55**, 4681.
7 Recent reviews: (a) A. Parra and S. Reboredo, *Chem. Eur. J.*, 2013, **19**, 17244; (b) F. Singh and T. Wirth, *Chem. Asian J.*, 2014, **9**, 950; (c) F. Berthiol, *Synthesis*, 2015, **47**, 587.
8 Recent examples: (a) S. J. Murray and H. Ibrahim, *Chem. Commun.* 2015, **51**, 2376; (b) D.-Y. Zhang, L. Xu, H. Wu, and L.-Z. Gong, *Chem.—Eur. J.*, 2015, **21**, 10314; (c) R. Coffinier, M. El Assal, P. A. Peixoto, C. Bosset, K. Miqueu, J.-M. Sotiropoulos, L. Pouységu, and S. Quideau, *Org. Lett.*, 2016, **18**, 1120; (d) K. Antien, G. Viault, L. Pouységu, P. A. Peixoto, and S. Quideau, *Tetrahedron*, 2017, **73**, 3684; (e) M. Ogasawara, H. Sasa, H. Hu, Y. Amano, H. Nakajima, N. Takenaga, K. Nakajima, Y. Kita, T. Takahashi, and T. Dohi, *Org. Lett.*, 2017, **19**, 4102; (f) M. Uyanik, N. Sasakura, M. Mizuno, and K. Ishihara, *ACS Catal.*, 2017, **7**, 872.
9 A. M. Harned, *Org. Biomol. Chem.*, 2018, **16**, 2324.
10 I. Colomer, C. Batchelor-McAuley, B. Odell, T. J. Donohoe, and R. G. Compton, *J. Am. Chem. Soc.* 2016, **138**, 8855.
11 Additional computational results using alternative functionals, basis sets, and solvation model that support this conclusion can be found in the ESI.
12 (a) C. D. Johnson *The Hammett Equation*, Cambridge University Press, London, 1973; (b) E. V. Anslyn and D. A. Dougherty, *Modern Physical Organic Chemistry*, University Science Books, Sausalito, CA, 2006, pp 445–453.
13 (a) A. S. Mitchell and R. A. Russell, *Tetrahedron*, 1997, **53**, 4387; (b) Y. Sawama, M. Masuda, R. Nakatani, H. Yokoyama, Y. Monguchi, T. Dohi, Y. Kita, and H. Sajiki, *Adv. Synth. Catal.*, 2016, **358**, 3683.
14 (a) H. M. Yau, A. K. Croft, and J. B. Harper, *Chem. Commun.* 2012, **48**, 8937; (b) H. M. Yau, R. S. Raines, and J. B. Harper, *J. Chem. Educ.* 2015, **92**, 538.
15 Other examples of Hammett studies using competitive rates: (a) J. H. Schauble, G. J. Walter, and J. G. Morin, *J. Org. Chem.*, 1974, **39**, 755; (b) H. Yamataka, T. Matsuyama, and T. Hanafusa, *J. Am.*

Chem. Soc., 1989, **111**, 4912; (c) R. J. Mullins, A. Vedernikov, and R. Viswanathan, *J. Chem. Educ.*, 2004, **81**, 1357; (d) P. Fristrup, S. Le Quement, D. Tanner, and P.-O. Norrby, *Organometallics*, 2004, **23**, 6160; (e) K. K. W. Mak, W.-F. Chan, K.-Y. Lung, W.-Y. Lam, W.-C. Ng, and S.-F. Lee, *J. Chem. Educ.*, 2007, **84**, 1819; (f) L. V. Desai, K. J. Stowers, and M. S. Sanford, *J. Am. Chem. Soc.*, 2008, **130**, 13285; (g) A. Bartoszewicz, G. González Miera, R. Marcos, P.-O. Norrby, and B. Martín-Matute, *ACS Catal.*, 2015, **5**, 3704; (h) A. L. Nash, R. Hertzberg, Y.-Q. Wen, B. Dahlgren, T. Brinck, and C. Moberg, *Chem. Eur. J.*, 2016, **22**, 3821.

16 See ESI for details.

17 Values for σ_p, σ^+, and σ^- were obtained from C. Hansch, A. Leo, and R. W. Taft, *Chem. Rev.*, 1991, **91**, 165. Values for σ_I and σ_R were obtained from M. Charton, *Prog. Phys. Org. Chem.*, 1981, **13**, 119.

18 H. H. Jaffé, *Chem. Rev.*, 1953, **53**, 191.

19 K. H. Pausacker, *J. Chem. Soc.*, 1953, 107.

20 J. March, *Advanced Organic Chemistry*, 4th Ed., Wiley, New York, 1992, pp 281.

21 Similar curvature was also seen when plotting the free energy change for the formation of the phenoxenium ion. See supporting information.